Generic Transverse Stability of Kink Structures in Atomic and Optical Nonlinear Media with Competing Attractive and Repulsive Interactions

S. I. Mistakidis,[1] G. Bougas,[1] G. C. Katsimiga,[1] and P. G. Kevrekidis[2,3]
[1]Department of Physics, Missouri University of Science and Technology, Rolla, Missouri 65409, USA
[2]Department of Mathematics and Statistics, University of Massachusetts Amherst, Amherst, Massachusetts 01003-4515, USA
[3]Department of Physics, University of Massachusetts Amherst, Amherst, Massachusetts, 01003, USA

(Received 11 June 2024; revised 15 January 2025; accepted 3 March 2025; published 26 March 2025)

We demonstrate the existence and stability of one-dimensional (1D) topological kink configurations immersed in higher-dimensional bosonic gases and nonlinear optical setups. Our analysis pertains, in particular, to the two- and three-dimensional extended Gross-Pitaevskii models with quantum fluctuations describing droplet-bearing environments but also to the two-dimensional cubic-quintic nonlinear Schrödinger equation containing higher-order corrections to the nonlinear refractive index. Contrary to the generic dark soliton transverse instability, the kink structures are generically robust under the interplay of low-amplitude attractive and high-amplitude repulsive interactions. A quasi-1D effective potential picture dictates the existence of these defects, while their stability is obtained numerically and analytically through linearization analysis and direct dynamics in the presence of external fluctuations showcasing their unprecedented resilience. These "generic" (across different models) findings should be detectable in current cold atom and optics experiments, offering insights toward controlling topological excitations.

DOI: 10.1103/PhysRevLett.134.123402

Introduction—Kink solitons (alias domain walls) are nonlinear excitations encountered in disparate disciplines ranging from optical [1] and magnetic media [2,3], living cellular structures [4–6], and folding protein chains [7,8] to atomic gases [9,10] and cosmology [11]. Their topological character has been recently unveiled in two-dimensional (2D) van der Waals materials [12], opening up the possibility of robust computations [13]. Stabilization of multidimensional spatially localized states is a fundamental challenge of scientific interest in physics and beyond [14]. It is well known that 1D topological (e.g., dark solitons) and nontopological (bright solitons) defects suffer from the so-called snake instability [15–18] and infrared catastrophe [19], respectively, once embedded in 2D and three-dimensional (3D) geometries. Mechanisms of suppression of the ensuing instabilities of defects have also been discussed. These mainly consider nonuniform media, i.e., incorporating external trapping geometries [20–22], or are accompanied by nonlocal interactions [23–25] or accounting for fractional dispersion in the presence of competing nonlinearities [26].

Cold atoms are ideal quantum many-body simulators, i.e., platforms featuring remarkable tunability of system parameters, such as, e.g., interactions and external traps [27,28]. In this context, ultradilute and incompressible self-bound states of matter, referred to as quantum droplets [29,30], were recently experimentally detected in Bose mixtures [31–35] and dipolar gases [36,37]. Stabilization of these states is achieved through the counterbalance of attractive and repulsive interactions modeled by mean-field nonlinear couplings and quantum fluctuations. The latter are incorporated perturbatively through the famous Lee-Huang-Yang (LHY) [38,39] correction whose sign and form depend on dimensionality [40] leading to an extended Gross-Pitaevskii equation (eGPE) [41,42]. These environments sustain also different kinds of nonlinear excitations such as dark solitons [43–45], bubbles [10,43], kinks [9,10,46], and vortices [47,48].

From a complementary nonlinear optics-seeded perspective, the cubic-quintic (CQ) model is an extension of the famous nonlinear Schrödinger model [49] constituting a universal mathematical toolbox involving higher-order nonlinearities. In the optical setting, the CQ model is utilized to study the propagation of electromagnetic waves [50,51] in photorefractive materials. In this context, the quintic term accounts for higher-order corrections to the nonlinear refractive index [52], i.e., incorporating susceptibilities up to fifth order. Experimentally, it is often also relevant to include the nontrivial (dissipative) absorption effects. The broad applicability of the CQ manifests by the fact that it has been deployed to describe various phenomena, for instance, liquid waveguides [50], special types of glasses [53], and colloids containing metallic nanoparticles [54]. In atomic gases, the cubic (quintic) coupling is related to the presence of two- (three-) body interactions [55–57] (see also, e.g., [58]).

In this Letter, we explore the dynamical transverse stability of kinks in a wide range of models from nonlinear optics and atomic physics, such as the 2D and 3D eGPE settings, as well as the 2D CQ model. A key feature of these

setups is the competition between attractive nonlinearities (dominant at low density) and repulsive ones (prevailing at high density) whose presence is crucial for the stability of kinks. Specifically, the stability and robustness of these entities is demonstrated in a threefold manner. First, we analytically extract and numerically evaluate the relevant for each model Bogoliubov–de Gennes (BdG) spectrum. Second, an analytical argument supporting kink's spectral stability against transverse modulations is constructed. Finally, we subject the relevant one-dimensional (1D) kink solutions to external, spatially distributed fluctuations (customarily present in experimental settings) and subsequently monitor their remarkable persistence for evolution times of the order of seconds. This demonstrates the relevance of these 1D topological defects in current state-of-the-art cold atom and nonlinear optics experiments and their structural robustness as potential information carriers. The topological character of the structures is evident in that no continuous, finite energy deformation can lead to their disappearance and that, accordingly, they preserve a form of topological charge invariant, given their distinct asymptotics at $\pm\infty$; see, e.g., [59,60] for details.

Models and theoretical analysis—To highlight the universal features of the existence and stability of kink solutions in higher spatial dimensions, three different nonlinear models characterized by competing attractive (at low density) and repulsive (at high density) interactions are investigated. These correspond to the eGPEs describing, for instance, self-bound quantum droplets in 2D [29,42] and 3D [29,41] and the CQ equation. Experimentally, the droplet-bearing systems can be emulated, e.g., by considering two hyperfine states of ^{39}K [32]. In optics, the CQ model is typically used to monitor, for instance, optical beam profiles of topological defects in liquid CS_2 [51]. In dimensionless form (see also Supplemental Material [61]), these equations read

$$i\partial_t\Psi = -\frac{1}{2}(\partial_x^2+\partial_y^2)\Psi + g|\Psi|^2\Psi\ln(|\Psi|^2), \tag{1a}$$

$$i\partial_t\Psi = -\frac{1}{2}(\partial_x^2+\partial_y^2)\Psi - |\Psi|^2\Psi + g_{\mathrm{CQ}}|\Psi|^4\Psi, \tag{1b}$$

$$i\partial_t\Psi = -\frac{1}{2}(\partial_x^2+\partial_y^2+\partial_z^2)\Psi + g_1|\Psi|^2\Psi + |\Psi|^3\Psi. \tag{1c}$$

Here, Eqs. (1a) and (1c) refer to the 2D and 3D eGPEs, while Eq. (1b) is the 2D CQ model with $g_{\mathrm{CQ}} > 0$. The right-hand side always contains the Laplacian and a nonlinear term where the latter can be written as $F(\Psi,\Psi^\star)$, using * to denote complex conjugation. In the 2D eGPE, the logarithmic nonlinearity encompasses both mean-field and first-order quantum fluctuation effects [29,42] of strength $g > 0$, while its 3D counterpart features a cubic (respectively, quartic) attractive with $g_1 < 0$ (respectively, repulsive) mean-field (LHY) contribution [41]; see also Supplemental Material [61]. Furthermore, in the CQ model there is an attractive (repulsive) cubic (quintic) nonlinear coupling commonly accounting for two- (three-) body interactions in the realm of cold gases [55,57] or higher-order corrections to the Kerr effect in nonlinear optics [51,52].

To infer the existence of planar kinks (i.e., one-dimensional ones embedded in higher dimensions), the following ansatz is employed: $\Psi(x,r_\perp,t) = e^{-i\mu t}u(x)$. Here, μ denotes the chemical potential and $r_\perp = y$ ($r_\perp = (y,z)$) are the transverse coordinates in 2D (3D). A uniform background is assumed along the transverse directions, and the $u(x)$ waveform is taken to be real without loss of generality. Introducing this ansatz into Eqs. (1a)–(1c) results in their reduced effective 1D time-independent standing wave analogs. These can be cast into Newtonian equations of motion, $d^2u(x)/dx^2 = -dV(u)/du$, subjected to the relevant for each model effective potential $V(u)$. These turn out to be

$$V_{2\mathrm{D}}(u) = \mu u^2 - g\frac{u^4}{2}\ln\left(\frac{u^2}{\sqrt{e}}\right), \tag{2a}$$

$$V_{2\mathrm{D}}(u) = \mu u^2 + \frac{u^4}{2} - g_{\mathrm{CQ}}\frac{u^6}{3}, \tag{2b}$$

$$V_{3\mathrm{D}}(u) = \mu u^2 - \frac{g_1}{2}u^4 - \frac{2}{5}u^5. \tag{2c}$$

Integration of the Newtonian equations of motion yields the effective energy E of the 1D reduced system [44]. While the resulting potentials feature multiple maxima, the frequency parameter μ can be generically tuned to render these maxima equienergetic, thus enabling a "genuine heteroclinic orbit," i.e., a kink, between $u = 0$ and $u = u_*$ with $E = 0$.

To systematically determine the finite kink backgrounds and chemical potentials, two conditions need to be satisfied, $V(u_*) = 0$ and $dV/du|_{u_*} = 0$, namely, conditions for the maximum at $u = u_*$ being equienergetic with the one at $u = 0$. The relevant solution for potentials

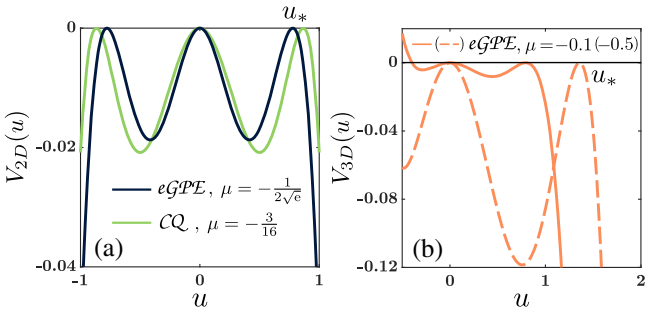

FIG. 1. Existence of kink configurations. Effective potential for the three nonlinear models: (a) 2D eGPE and CQ models with $g = g_{\mathrm{CQ}} = 1$ as well as (b) the 3D eGPE setup with $g_1 = -0.952$ ($g_1 = -1.629$) for $\mu = -0.1$ ($\mu = -0.5$). The effective potentials host the kink configuration, whose wave function is constrained within 0 and u_*. These states occur at specific chemical potentials (see legends).

with a competing set of interactions yields μ and u_* of the kink. The solution exists provided that the attractive and repulsive potentials grow faster than the quadratic power of the chemical potential term within V and that the repulsive contribution dominates the attractive as $u \to \infty$. For the 2D eGPE (CQ) these values lead analytically to $\mu = -g/(2\sqrt{e})$, $u_* = e^{-1/4}$ [$\mu = -3/(16 g_{\rm CQ})$ and $u_* = \sqrt{3/(4 g_{\rm CQ})}$] [Fig. 1(a)]. The u_* boundary for the 2D eGPE separates the parameter region of droplets from that of 2D bubbles [29,42], analogous to what is the case also in 1D [10]. For the 3D eGPE, the chemical potential and extremum are $\mu = 25 g_1^3/216$ and $u_* = -5 g_1/6$, respectively [Fig. 1(b)]. Notice that, while such kink-type states have been discussed for CQ settings previously (see, e.g., [72]), they are unprecedented, to our knowledge, for the emergent atomic theme of 2D and 3D quantum droplet settings. Interestingly, the asymmetry of the effective potential $V_{\rm 3D}(u)$ [Fig. 1(b)] suggests the concurrent existence of a heretofore unexplored quantum droplet (for values of $u < 0$) whose analysis is deferred for future studies.

Within the effective potential framework, unique kink solutions exist for each coupling strength when competing interactions exist, i.e., when $g_{\rm CQ} > 0$ and $g_1 < 0$. Otherwise, for $g_{\rm CQ} \leq 0$ and $g_1 \geq 0$ kink configurations do not exist as dictated by the effective potentials of Eqs. (2b) and (2c), respectively; see also Supplemental Material [61]. In what follows, without loss of generality g and $g_{\rm CQ}$ are set to unity in order to inspect the stability properties of these topological defects. On the other hand, the mean-field interaction g_1 in the 3D eGPE is routinely tunable in experiments via Feshbach resonances; see Ref. [32] and Supplemental Material [61]. Stability of the kink can also be ensured for other values of the interaction coefficients in the 3D eGPE and 2D CQ models as long as there is an active attractive-repulsive interplay; see for details Supplemental Material [61].

Spectral stability of kinks in higher dimensions—According to the aforementioned effective potential description, the 1D planar kink solution occurs for $\mu = -1/(2\sqrt{e})$, $\mu = -3/16$, and, e.g., $\mu = -0.115$ where $g_1 = -1$, within the 2D eGPE, 2D CQ, and 3D eGPE models, respectively. The relevant effective 1D but also the higher-dimensional stationary states are obtained upon utilizing heteroclinic (tanh-shaped) initial guesses, bearing the correct asymptotics. In the CQ case, an analytical form exists, $u = \sqrt{\frac{3}{8}[1 + \tanh(\sqrt{3}x/2\sqrt{2})]}$ [72,73]. Naturally, such 1D planar waveforms satisfy the corresponding 2D and 3D time-independent version of Eqs. (1a)–(1c).

To extract the stability properties of these configurations, small perturbations of the numerically exact (up to a prescribed tolerance) kink solutions are considered having the form $\Psi = (\Psi_0 + \epsilon a e^{-i\omega t} + \epsilon b^\star e^{i\omega^\star t}) e^{-i\mu t}$. a, b (ω) refer to the eigenvectors (eigenfrequencies), while $\epsilon \ll 1$ is a small perturbation parameter. Utilizing this ansatz and keeping terms of order $\mathcal{O}(\epsilon)$ leads to an eigenvalue problem that, irrespective of the system under consideration [Eqs. (1a)–(1c)], can be written as

$$\begin{bmatrix} \hat{L}_{11} & \hat{L}_{12} \\ \hat{L}_{21} & \hat{L}_{22} \end{bmatrix} \begin{bmatrix} a \\ b \end{bmatrix} = \omega \begin{bmatrix} a \\ b \end{bmatrix}. \tag{3}$$

The model-dependent diagonal matrix elements are $\hat{L}_{11} = -\frac{1}{2}\nabla^2 - \mu + \Psi_0^2 + 2\Psi_0^2 \ln(\Psi_0^2)$, $\hat{L}_{11} = -\frac{1}{2}\nabla^2 - \mu - 2\Psi_0^2 + 3\Psi_0^4$, and $\hat{L}_{11} = -\frac{1}{2}\nabla^2 - \mu + 2g_1\Psi_0^2 + \frac{5}{2}\Psi_0^3$, for the 2D eGPE, CQ, and 3D eGPE models, respectively. Their relevant off-diagonal counterparts read $\hat{L}_{12} = \Psi_0^2 + \Psi_0^2 \ln(\Psi_0^2)$, $\hat{L}_{12} = -\Psi_0^2 + 2\Psi_0^4$, and $\hat{L}_{12} = g_1\Psi_0^2 + \frac{3}{2}\Psi_0^3$, respectively. In all cases, $\hat{L}_{11} = -\hat{L}_{22}$, $\hat{L}_{12} = -\hat{L}_{21}$, and ∇^2 denotes the $\mathcal{N}$-dimensional Laplace operator. Additionally, Ψ_0 designates the stationary, real kink state for each distinct model.

The stability analysis outcome for all three models is depicted in Figs. 2(a)–2(c). In all scenarios, spectral stability of the kink state can be inferred from the *absence* of a finite imaginary part, $\mathrm{Im}(\omega) \sim 10^{-12}$, in the pertinent BdG spectrum. For all settings, the first hundred eigenvalues of the continuous quasi-1D BdG spectra are illustrated, while we verified that their relevant higher-dimensional analogs produce the same stability result. For the quasi-1D BdG spectra, the transverse direction is decomposed into Fourier modes with the "quantization" thereof from a finite transverse computational domain accounted for. The stability of a plethora of effective 1D spectra for different transverse wave numbers is confirmed.

Moreover, an analytical argument for the kinks stability relies on an alternative BdG formulation, utilizing the perturbation $\Psi(x, r_\perp, t) = [\tilde{u}(x) + w(x, r_\perp, t)] e^{-i\mu t}$, where

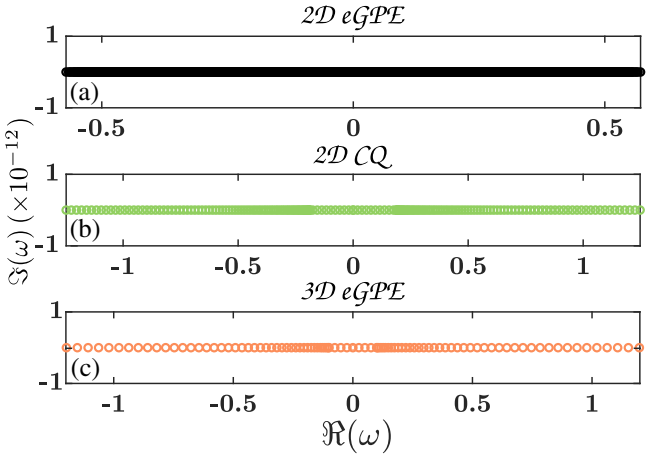

FIG. 2. Spectral stability of kinks. BdG analysis for the kink waveforms within (a) the 2D eGPE, (b) 2D CQ, and (c) the 3D eGPE models. The absence of a finite imaginary part, $\mathrm{Im}[\omega] \neq 0$, in the spectrum showcases the stability of the respective kink states.

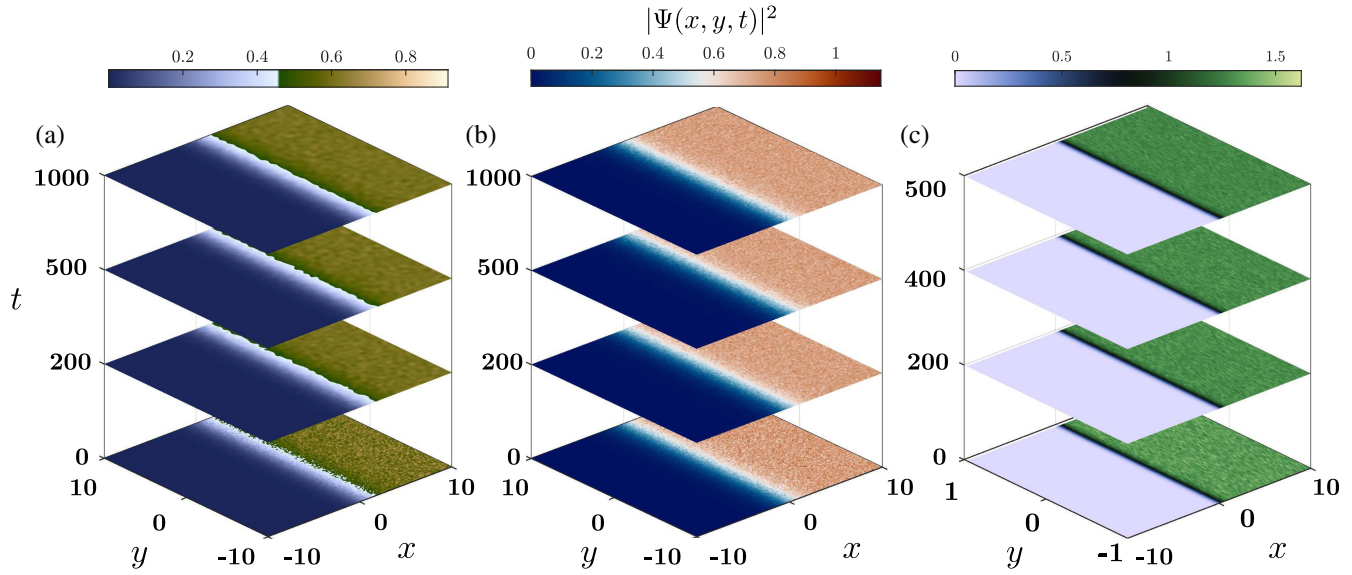

FIG. 3. Resilience of kink states. Density snapshots depicting the evolution of perturbed kink solutions within the (a) 2D eGPE, (b) CQ, and (c) 3D eGPE models with $\mu = -0.1$. It can be readily seen that, in all cases, the kink is robust throughout the evolution with its core remaining intact and the waveform maintaining its shape despite being significantly distorted due to external spatial and phase fluctuations. The box sizes used for the simulations correspond to $L_x = L_y = 400$ and $L_z = 6$.

w is a complex wave function (see also Supplemental Material [61]). Here, stability is determined by the spectral operators $L_{\pm,0} = -\frac{1}{2}\partial_x^2 - \mu + [\partial F(u,u^\star)/\partial u]|_{\tilde{u}} \pm [\partial F(u,u^\star)/\partial u^\star]|_{\tilde{u}}$ at transverse wave number $k_\perp = 0$, where $\tilde{u}$ is the relevant kink solution. Direct calculation yields $L_{+,0}(\partial_x\tilde{u}) = 0$ and since $\partial_x\tilde{u}$ is nodeless, according to the Sturm-Liouville theorem, it is the ground state of $L_{+,0}$ with eigenvalue $\lambda = 0$. Similarly, $L_{-,0}\tilde{u} = 0$ leading $\tilde{u}$ to be an eigenfunction of the latter operator with $\lambda = 0$. This, together with the addition of $k_\perp^2/2$ for transverse modulations $\propto e^{ik_\perp r_\perp}$ implies that the spectra of the operators $L_{\pm,k_\perp} = L_{\pm,0} + k_\perp^2/2$ are non-negative. Then, a straightforward spectral argument (provided in Supplemental Material [61]) rigorously proves that there are no exponentially growing transverse modulations of finite $k_\perp$, which can destabilize the kink, as further verified by our simulations below.

Dynamical confirmation of the absence of transverse instability for the kinks—To corroborate our BdG findings, we next consider the dynamical evolution of the stationary kink solution for each of the models under study. Specifically, we aim not only to mimic unavoidable experimental imperfections but also to exemplify the robust nature of the kink structure in the presence of transverse perturbations. To that effect, the kink initial state is significantly perturbed via a random normal distribution generator $\delta(x, r_\perp)$. The ensuing wave function acquires the form $\psi(x, r_\perp, t = 0) = \Psi_0[1 + \varepsilon\delta(x, r_\perp)]$. In this context, $\delta(x, r_\perp)$ is characterized by zero mean and unit variance, while $\varepsilon = \varepsilon_R + i\varepsilon_I$ such that also phase disturbances are encountered. This implies that both the core and the background of the kink are perturbed with the latter accounting for chemical potential (particle number) fluctuations unavoidable in experiments. The same holds upon considering perturbations in the interaction coefficients (not shown for brevity). In particular, the considered amplitudes of the perturbation range lie in the interval $[10\%, 50\%]$ of the solution amplitude. Typical evolution times (in the dimensionless units adopted herein) are of the order of $\sim$500 and $\sim 10^3$ for the 3D and 2D settings, respectively, confirming the longevity of these planar 1D defects upon their exposure to transverse excitations.

Evidently, despite the significantly excited nature of the initial state, the kink remains intact preserving its shape throughout the evolution, while "shedding" some of the relevant "radiation" in the form of dispersive wave packets, as can be seen in Figs. 3(a)–3(c). Particularly here, distinct plates correspond to density, $|\Psi(x, y, t)|^2$, contours in the $x - y$ plane taken at different times during the propagation of the perturbed kink configuration. For the 3D dynamics, the z direction is integrated out, while we note that the robustness of the kink configurations has also been verified for different values of the chemical potential and hence distinct interaction strengths.

Experimental implications—For droplet-bearing settings, two hyperfine levels, e.g., $|F = 1, m_F = 0\rangle$ and $|F = 1, m_F = -1\rangle$ of ultracold ^{39}K in the vicinity of the 59 G intraspecies Feshbach resonance [62,74] feature competing intra- and interspecies interactions [32,33]. They are experimentally populated using radio frequency spectroscopy [33] and their dynamics can be adequately described by the eGPE models [Eqs. (1a) and (1c)] in 2D and 3D. For the 3D setup with averaged mean-field scattering length $\delta a = -0.24a_0$, propagation times

of the kink (∼500 in dimensionless units) refer approximately to 800 m s [61]. The corresponding 2D pancake geometry features a tight harmonic trap along one spatial dimension [75] and, e.g., for $\omega_z = 2\pi \times 2$ kHz [33,63] and $\delta a = -1.5 a_0$ (see Supplemental Material [61]), the relevant timescale (∼1000 in dimensionless units) for the kink evolution is 2 sec. These long evolution times guarantee the resilience of the kink in current state-of-the-art experiments incurring additionally three-body recombination [32].

On the other hand, the 2D CQ equation is used to describe, for instance, propagation of electromagnetic waves in optical media incorporating higher-order nonlinear refractive indices [76]. Characteristic materials featuring such properties are chalcogenide glasses [53], such as liquid CS_2 [50,51]. In these setups (where optical vortices and their destabilization has been monitored [77]), the time evolution is probed by measuring the transmission of the kink along the axial direction of the nonlinear medium. Considering a light beam of 900 nm [50], a propagation distance of 10^3 corresponds to 0.14 mm axial depth for the kink transmission. Finally, in either cold bosonic mixtures or nonlinear optical media, kink defects can be imprinted in the bulk by means of the well-established technique of density engineering [18,64,65,78] or by utilizing digital micromirror device patterned optical traps [63,79–81]. In the Supplemental Material [61], we demonstrate the kink dynamical formation through density engineering and its potential robustness under different trap settings.

Conclusions and future challenges—The existence and corresponding spectral and dynamical stability of 1D kink solutions embedded in higher-dimensional gases or nonlinear optical media featuring competing attractive lower-order and repulsive higher-order interactions is unveiled. To establish the breadth and generality of results, this is exemplarily demonstrated for three representative models, the 2D and 3D eGPE droplet-bearing systems and the 2D CQ setting relevant in nonlinear optics. We explicated the existence of these 1D topological defects upon analytically extracting, in each case, a quasi-1D effective potential picture, subsequently supplemented by their spectral stability inferred through linearization analysis, both numerically and analytically. Additionally, monitoring their dynamical evolution in the presence of external fluctuations revealed their profound robustness and resilience, for times up to few seconds.

These results suggest the use of kink defects as promising candidates for topological quantum computing. Indeed, contrary to the generically transversely unstable dark soliton states [17], kinks appear to defy the proneness to transverse modulations. Importantly, also, these results pave the way for further physical and mathematical studies. Our effective potential analysis suggests the existence of further lower-dimensional nonlinear excitations (including droplets, bubbles, etc.), whose transverse dynamics and potential dynamical features may be of further theoretical and experimental interest in their own right.

Acknowledgments—We acknowledge fruitful discussions with B. Malomed and we are grateful to J. Holmer for extensive discussions and insights regarding the analytical treatment of the kink stability. We also thank the anonymous referee for the insightful comments. This material is based upon work supported by the U.S. National Science Foundation under Awards No. PHY-2110030, No. PHY-2408988, and No. DMS-2204702 (P. G. K.). S. I. M. acknowledges support from the Missouri University of Science and Technology, Department of Physics, Startup fund.

[1] Y. V. Kartashov, V. A. Vysloukh, and L. Torner, Opt. Express **14**, 12365 (2006).
[2] A. Pérez-Junquera, V. Marconi, A. B. Kolton, L. Álvarez-Prado, Y. Souche, A. Alija, M. Vélez, J. V. Anguita, J. Alameda, J. I. Martín, and J. M. R. Parrondo, Phys. Rev. Lett. **100**, 037203 (2008).
[3] F. J. Buijnsters, A. Fasolino, and M. I. Katsnelson, Phys. Rev. Lett. **113**, 217202 (2014).
[4] V. G. Ivancevic and T. T. Ivancevic, J. Geom. Symmetry Phys. **31**, 1 (2013).
[5] S. Yomosa, Phys. Rev. A **27**, 2120 (1983).
[6] S. Caspi and E. Ben-Jacob, Europhys. Lett. **47**, 522 (1999).
[7] S. Hu, M. Lundgren, and A. J. Niemi, Phys. Rev. E **83**, 061908 (2011).
[8] S. Hu, A. Krokhotin, A. J. Niemi, and X. Peng, Phys. Rev. E **83**, 041907 (2011).
[9] M. Tylutki, G. E. Astrakharchik, B. A. Malomed, and D. S. Petrov, Phys. Rev. A **101**, 051601(R) (2020).
[10] G. C. Katsimiga, S. I. Mistakidis, B. A. Malomed, D. J. Frantzeskakis, R. Carretero-Gonzalez, and P. G. Kevrekidis, Condens. Matter **8**, 67 (2023).
[11] A. Vilenkin and E. P. S. Shellard, *Cosmic Strings and Other Topological Defects* (Cambridge University Press, Cambridge, England, 2000).
[12] J. Lee, J. W. Park, G. Y. Cho, and H. W. Yeom, Adv. Mater. **35**, 2300160 (2023).
[13] I.-T. Wang, C.-C. Chang, Y.-Y. Chen, Y.-S. Su, and T.-H. Hou, Neuromorph. Comput. Eng. **2**, 012003 (2022).
[14] Y. V. Kartashov, G. E. Astrakharchik, B. A. Malomed, and L. Torner, Nat. Rev. Phys. **1**, 185 (2019).
[15] V. Tikhonenko, J. Christou, B. Luther-Davies, and Y. S. Kivshar, Opt. Lett. **21**, 1129 (1996).
[16] A. V. Mamaev, M. Saffman, and A. A. Zozulya, Phys. Rev. Lett. **76**, 2262 (1996).
[17] Y. S. Kivshar and D. E. Pelinovsky, Phys. Rep. **331**, 117 (2000).
[18] B. P. Anderson, P. C. Haljan, C. A. Regal, D. L. Feder, L. A. Collins, C. W. Clark, and E. A. Cornell, Phys. Rev. Lett. **86**, 2926 (2001).
[19] G. Fibich, *The Nonlinear Schrödinger Equation* (Springer, New York, 2015), Vol. 192.

[20] N. Proukakis, N. Parker, D. Frantzeskakis, and C. Adams, J. Opt. B **6**, S380 (2004).
[21] W. Wen, C. Zhao, and X. Ma, Phys. Rev. A **88**, 063621 (2013).
[22] P. G. Kevrekidis, G. Theocharis, D. J. Frantzeskakis, and A. Trombettoni, Phys. Rev. A **70**, 023602 (2004).
[23] S. Skupin, O. Bang, D. Edmundson, and W. Krolikowski, Phys. Rev. E **73**, 066603 (2006).
[24] Y. Lin, R.-K. Lee, and Y. S. Kivshar, J. Opt. Soc. Am. B **25**, 576 (2008).
[25] R. Nath, P. Pedri, and L. Santos, Phys. Rev. Lett. **101**, 210402 (2008).
[26] L. Zeng and J. Zeng, Commun. Phys. **3**, 26 (2020).
[27] I. Bloch, J. Dalibard, and W. Zwerger, Rev. Mod. Phys. **80**, 885 (2008).
[28] M. Lewenstein, A. Sanpera, and V. Ahufinger, *Ultracold Atoms in Optical Lattices: Simulating quantum many-body systems* (Oxford University Press, Oxford, 2012).
[29] Z.-H. Luo, W. Pang, B. Liu, Y.-Y. Li, and B. A. Malomed, Front. Phys. **16**, 1 (2021).
[30] S. I. Mistakidis, A. G. Volosniev, R. E. Barfknecht, T. Fogarty, T. Busch, A. Foerster, P. Schmelcher, and N. T. Zinner, Phys. Rep. **1042**, 1 (2023).
[31] P. Cheiney, C. R. Cabrera, J. Sanz, B. Naylor, L. Tanzi, and L. Tarruell, Phys. Rev. Lett. **120**, 135301 (2018).
[32] G. Semeghini, G. Ferioli, L. Masi, C. Mazzinghi, L. Wolswijk, F. Minardi, M. Modugno, G. Modugno, M. Inguscio, and M. Fattori, Phys. Rev. Lett. **120**, 235301 (2018).
[33] C. R. Cabrera, L. Tanzi, J. Sanz, B. Naylor, P. Thomas, P. Cheiney, and L. Tarruell, Science **359**, 301 (2018).
[34] C. D'Errico, A. Burchianti, M. Prevedelli, L. Salasnich, F. Ancilotto, M. Modugno, F. Minardi, and C. Fort, Phys. Rev. Res. **1**, 033155 (2019).
[35] A. Burchianti, C. D'Errico, M. Prevedelli, L. Salasnich, F. Ancilotto, M. Modugno, F. Minardi, and C. Fort, Condens. Matter **5**, 21 (2020).
[36] L. Chomaz, I. Ferrier-Barbut, F. Ferlaino, B. Laburthe-Tolra, B. L. Lev, and T. Pfau, Rep. Prog. Phys. **86**, 026401 (2023).
[37] F. Böttcher, J.-N. Schmidt, J. Hertkorn, K. S. H. N g, S. D. Graham, M. Guo, T. Langen, and T. Pfau, Rep. Prog. Phys. **84**, 012403 (2020).
[38] T. D. Lee, K. Huang, and C. N. Yang, Phys. Rev. **106**, 1135 (1957).
[39] D. M. Larsen, Ann. Phys. (N.Y.) **24**, 89 (1963).
[40] T. Ilg, J. Kumlin, L. Santos, D. S. Petrov, and H. P. Büchler, Phys. Rev. A **98**, 051604(R) (2018).
[41] D. S. Petrov, Phys. Rev. Lett. **115**, 155302 (2015).
[42] D. S. Petrov and G. E. Astrakharchik, Phys. Rev. Lett. **117**, 100401 (2016).
[43] M. Edmonds, Phys. Rev. Res. **5**, 023175 (2023).
[44] G. C. Katsimiga, S. I. Mistakidis, G. N. Koutsokostas, D. J. Frantzeskakis, R. Carretero-González, and P. G. Kevrekidis, Phys. Rev. A **107**, 063308 (2023).
[45] S. Saqlain, T. Mithun, R. Carretero-González, and P. G. Kevrekidis, Phys. Rev. A **107**, 033310 (2023).
[46] Y. V. Kartashov, V. M. Lashkin, M. Modugno, and L. Torner, New J. Phys. **24**, 073012 (2022).
[47] Y. Li, Z. Chen, Z. Luo, C. Huang, H. Tan, W. Pang, and B. A. Malomed, Phys. Rev. A **98**, 063602 (2018).
[48] T. A. Yoğurt, U. Tanyeri, A. Keleş, and M. O. Oktel, Phys. Rev. A **108**, 033315 (2023).
[49] R. Killip, T. Oh, O. Pocovnicu, and M. Vişan, Arch. Ration. Mech. Anal. **225**, 469 (2017).
[50] E. L. Falcão Filho, C. B. de Araújo, G. Boudebs, H. Leblond, and V. Skarka, Phys. Rev. Lett. **110**, 013901 (2013).
[51] A. S. Reyna, H. T. M. C. M. Baltar, E. Bergmann, A. M. Amaral, E. L. Falcão Filho, P.-F. m. c. Brevet, B. A. Malomed, and C. B. de Araújo, Phys. Rev. A **102**, 033523 (2020).
[52] N. Akhmediev and V. V. Afanasjev, Phys. Rev. Lett. **75**, 2320 (1995).
[53] G. Boudebs, S. Cherukulappurath, H. Leblond, J. Troles, F. Smektala, and F. Sanchez, Opt. Commun. **219**, 427 (2003).
[54] E. Falcão-Filho, C. B. de Araújo, and J. Rodrigues Jr, J. Opt. Soc. Am. B **24**, 2948 (2007).
[55] E. K. Luckins and R. A. Van Gorder, Ann. Phys. (Amsterdam) **388**, 206 (2018).
[56] W. B. Cardoso, A. T. Avelar, and D. Bazeia, Phys. Rev. E **83**, 036604 (2011).
[57] A. Bulgac, Phys. Rev. Lett. **89**, 050402 (2002).
[58] E. B. Kolomeisky, T. J. Newman, J. P. Straley, and X. Qi, Phys. Rev. Lett. **85**, 1146 (2000).
[59] N. Manton and P. Sutcliffe, *Topological Solitons* (Cambridge University Press, Cambridge, England, 2004).
[60] S. Coleman, Classical lumps and their quantum descendants, in *New Phenomena in Subnuclear Physics: Part A*, edited by A. Zichichi (Springer US, Boston, MA, 1977), pp. 297–421.
[61] See Supplemental Material at http://link.aps.org/supplemental/10.1103/PhysRevLett.134.123402 for more information regarding further analytical arguments about the kink stability, additional excitation spectra unveiling stability, density engineering, and the dimensional expressions of the nonlinear models, as well as the relation with physical parameters, which includes Refs. [62–71].
[62] C. Chin, R. Grimm, P. Julienne, and E. Tiesinga, Rev. Mod. Phys. **82**, 1225 (2010).
[63] R. Saint-Jalm, P. C. M. Castilho, E. Le Cerf, B. Bakkali-Hassani, J.-L. Ville, S. Nascimbene, J. Beugnon, and J. Dalibard, Phys. Rev. X **9**, 021035 (2019).
[64] A. Farolfi, D. Trypogeorgos, C. Mordini, G. Lamporesi, and G. Ferrari, Phys. Rev. Lett. **125**, 030401 (2020).
[65] I. Shomroni, E. Lahoud, S. Levy, and J. Steinhauer, Nat. Phys. **5**, 193 (2009).
[66] G. Bougas, G. C. Katsimiga, P. G. Kevrekidis, and S. I. Mistakidis, Phys. Rev. A **110**, 033317 (2024).
[67] G. B. Arfken, H.-J. Weber, and F. E. Harris, *Mathematical methods for Physicists: A Comprehensive Guide* (Academic Press, 1972), ISBN-13 978-0123846549.
[68] S. R. Otajonov, E. N. Tsoy, and F. K. Abdullaev, Phys. Rev. E **102**, 062217 (2020).
[69] M. Abramowitz, I. A. Stegun, and R. H. Romer, *Handbook of Mathematical Functions with Formulas, Graphs, and Mathematical Tables* (US Government printing office, Washington DC, 1988), Vol. 55.
[70] D. S. Petrov and G. V. Shlyapnikov, Phys. Rev. A **64**, 012706 (2001).

[71] D. S. Petrov, M. Holzmann, and G. V. Shlyapnikov, Phys. Rev. Lett. **84**, 2551 (2000).
[72] Z. Jin-Liang, W. Ming-Liang, and L. Xiang-Zheng, Commun. Theor. Phys. **45**, 343 (2006).
[73] Z. Birnbaum and B. A. Malomed, Physica (Amsterdam) **237D**, 3252 (2008).
[74] C. D'Errico, M. Zaccanti, M. Fattori, G. Roati, M. Inguscio, G. Modugno, and A. Simoni, New J. Phys. **9**, 223 (2007).
[75] Z. Hadzibabic and J. Dalibard, Riv. Nuovo Cimento Soc. Ital. Fis. **34**, 389 (2011).
[76] R. L. Sutherland, *Handbook of Nonlinear Optics* (CRC Press, Boca Raton, 2003), 10.1201/9780203912539.
[77] A. S. Desyatnikov, Y. S. Kivshar, and L. Torner, Prog. Opt. **47**, 291 (2005).
[78] M. R. Matthews, B. P. Anderson, P. C. Haljan, D. S. Hall, C. E. Wieman, and E. A. Cornell, Phys. Rev. Lett. **83**, 2498 (1999).
[79] N. Navon, R. P. Smith, and Z. Hadzibabic, Nat. Phys. **17**, 1334 (2021).
[80] G. Gauthier, I. Lenton, N. M. Parry, M. Baker, M. Davis, H. Rubinsztein-Dunlop, and T. Neely, Optica **3**, 1136 (2016).
[81] H. Tamura, C.-A. Chen, and C.-L. Hung, Phys. Rev. X **13**, 031029 (2023).